

Essential oil from *Euphorbia esula* inhibits proliferation and induces apoptosis in HepG2 cells via mitochondrial dysfunction

Dan Lv^{1#}, Li-hong Pan^{2#}, Ren Zhang¹, Jie Yang³, Hao Chen³, Yanzhang Wen³, Mi Huang³,
Xinhua Ma³, Qiang Wang^{1*}, Xinzhou Yang^{3*}

¹Institute of Infection, Immunology and Tumor Microenvironment, Hubei Province Key Laboratory of Occupational Hazard Identification and Control, Medical College, Wuhan University of Science and Technology, Wuhan, China, ²College of Basic Medicine and Forensic Medicine of Hangzhou Medical College, ³School of Pharmaceutical Sciences, South-Central University for Nationalities, Wuhan, China

Hepatocellular carcinoma is one of the most prevalent malignancies and a leading cause of cancer-related mortality worldwide. However, the therapies to prevent hepatocellular carcinoma are still limited and the emergence of drug resistance leads to the development of new anti-cancer drugs and combinational chemotherapy regimens. Our study was aimed to explore the anticancer effects of the essential oil extract (EEEE) from *Euphorbia esula* which has been widely used in traditional Chinese folk medicine and possessed potential cytotoxic effects in several human tumor cells. However, the mechanisms of EEEO-induced anti-proliferation and apoptosis have not been completely elucidated. In this study, EEEO was prepared by hydro-distillation and the main chemical component of EEEO was identified by GC-MS. HepG2 cells were treated with EEEO *in vitro* and then evaluated with respect to proliferation, apoptosis, and levels of reactive oxygen species (ROS) and apoptotic proteins. Our studies showed that EEEO decreased cell viability, elevated ROS levels, and induced apoptosis of HepG2 cells in a concentration- and time-dependent manner. Furthermore, Bcl-2 was down-regulated, while Bax was up-regulated in HepG2 after EEEO treatment. These results suggest that EEEO induced apoptosis of HepG2 cells and indicate that this apoptosis might be mediated by the mitochondrial pathway.

Keywords: *Euphorbia esula*. Hepatocellular carcinoma. Apoptosis. Reactive oxygen species. Mitochondrial pathway.

INTRODUCTION

Hepatocellular carcinoma (HCC), the most common primary malignant tumor of the liver, has become a serious threat to human health worldwide (Santos *et al.*, 2015; Lv *et al.*, 2017). China has the highest incidence and mortality of liver cancer in the world. It is estimated that 55% of liver cancer cases occurred in China alone compared to the rest of the developing countries in 2010 (Wei *et al.*, 2014). Surgery, chemotherapy and radiotherapy are the three most common strategies used for the treatment of HCC (Hong *et al.*, 2015). Although

drug therapy remains the mainstay in the treatment of liver cancer, traditional chemotherapy drugs in clinical application currently suffer from lack of selectivity and wide distribution in the body. As a result, these drugs often produce toxic side effects including severe systemic effects, such as myelosuppression (leukopenia, immune suppression, fatigue), digestive tract epithelial cell toxicity (nausea and vomiting) and hair cell toxicity (hair loss), affecting the efficacy of chemotherapy (Li, Ling, 2012). Therefore, identification of novel anticancer agents with high therapeutic effects but less toxic effects has become a key issue in the search for innovative drugs for the treatment of HCC (Song *et al.*, 2015a).

Euphorbia esula is a perennial herbaceous plant of Euphorbiaceae (Chen, Gilbert, 2006). It grows in the hillside, valley grassland, and sandy ground, reaching about 30 ~ 60 cm in height, and is widely distributed in China (Ernst *et al.*, 2015). It has long been used for the

*Correspondence: Q. Wang. Institute of Infection Immunology and Tumor Microenvironment, Hubei Province Key Laboratory of Occupational Hazard Identification and Control, Medical College, Wuhan University of Science and Technology, Wuhan 430065, China. E-mail: wangqiang@wust.edu.cn
X.Z. Yang. School of Pharmaceutical Sciences, South-Central University for Nationalities, Wuhan, China. E-mail: xzyang@mail.scuec.edu.cn. #Authors contributed equally to this work.

treatment of swollen limbs, difficulty in urination, enteritis, malaria, and chronic tracheitis in clinical practice. In addition, *E. esula* has been shown to have a good topical curative effect on cervical lymphoid tuberculosis, ringworm sores, and itching. As a traditional Chinese folk medicine, *E. esula* was generally used for the treatment of swelling and warts, but seldom used for the treatment of malignant tumors, especially in hepatocellular carcinoma.

In this study, we report that EEEO has the potential to induce apoptosis in HCC cells. In addition, we also identified 13 chemical components from *E. esula* by GC-MS analysis, validated the potential anti-HCC effects of EEEO *in vitro*, and elucidated its likely anti-HCC mechanism through the mitochondrial pathway.

MATERIAL AND METHODS

Material and equipment

Dulbecco's Modified Eagle Medium (DMEM) and fetal bovine serum (FBS) were purchased from Life Technologies Corporation (USA). 3-(4,5-dimethylthiazol-2-yl)-2,5-diphenyltetrazoliumbromide (MTT) and dimethyl sulphoxide (DMSO) were obtained from Sigma (USA). The antibodies for Bcl-2, Bax, Caspase-3, Caspase-9, and β -actin were obtained from Cell Signaling Technology (USA). Cell Apoptosis PI Detection Kit was purchased from BD Pharmingen (China). Protein assay kits (BCA) and reactive oxygen species (ROS) were bought from Beyotime Biotechnology (China). The chemical reagents were purchased from Sinopharm Chemical Reagent Co. Ltd. (China). The HPLC grade methanol and acetonitrile were purchased from Tedia (USA). Enzyme standard instrument was purchased from American Bio Rad 3550.

Plant material and preparation of EEEO

The whole plants of *Euphorbia esula* were collected on 16 August, 2013 in Wufeng County, Hubei province, China, and identified by Professor Dingrong Wan at School of Pharmaceutical Sciences, South-Central University for Nationalities (SCUN), Wuhan, China. A voucher Specimen (No. SC0034) is deposited in the Herbarium of School of Pharmaceutical Sciences, SCUN. Air-dried whole plants of *E. esula* (450 g) were boiled with distilled water (3 × 3500 mL, 3 h each) to yield crude essential oil in a 3 L round bottom flask fitted with a volatile oil distillation apparatus (Yang *et al.*, 2016). The obtained residue was extracted with cyclohexane, then dried with anhydrous sodium sulfate and filtered to yield the EEEO

(4.7 mL). The resulting EEEO was stored at 4 °C prior to further analyses and bioassay.

GC-MS analysis of EEEO

An Agilent gas chromatography-mass spectrometer (7890N/5973iN) coupled with a HP 5975C mass spectrometer (Agilent Technologies, USA) and a HP-5MS capillary column (30 m × 0.25 mm id; 0.25 μ m film thickness) was used for the chemical analysis of EEEO (Yang *et al.*, 2017). Helium gas was used as a carrier gas with a flow rate of 1.2 mL/min. The ionization energy was set at 70 eV with an acquisition range between 50 and 800 m/z and a scan rate of 1 scan/s. The composition was reported as a relative percentage of the total peak area. Injector and detector temperatures were set at 250 °C and 280 °C, respectively. The oven temperature was initially maintained at 50 °C, then increased to 150 °C at 5 °C/min, and finally increased to 300 °C at 15 °C/min with a 10 min hold. EEEO was dissolved in diethylether, and 0.2 μ L of the diluted sample was injected manually. The chemical components were identified based on the comparison of their relative retention time and their mass spectra with those in the NIST08 database.

Cell culture

Human carcinoma cell lines HepG2, Hep3B, Huh7, SMMC-7721 and normal hepatocyte cell line L0-2 were purchased from the American Type Culture Collection (ATCC, Manassas, VA). These cells were inoculated in DMEM (Gibco) with 10% fetal bovine serum (FBS), 100 U/mL penicillin and 100 mg/L streptomycin at 37 °C and 5% CO₂, in a humid condition.

MTT assay

Cell viability and cytotoxicity was determined using the 3-(4, 5-dimethylthiazol-2-yl)-2,5-diphenyltetrazolium bromide (MTT) assay (Stepanenko *et al.*, 2015; Song *et al.*, 2015 b). For the treatment, EEEO was dissolved in DMSO to make a stock solution of 200 mg/mL and further diluted to final concentrations of 0, 25, 50, 100, 150 and 200 μ g/mL with serum-free culture medium containing 1% DMSO (Li *et al.*, 2016). The logarithmic phase cells (HepG2, Hep3B, Huh7, SMMC-7721 and L0-2) were cultured in the 96-well plates at a concentration of 1 × 10⁵ cells/mL (100 μ L/well), and treated in triplicate with various concentration of EEEO for 24 h. Then, 20 μ L (5 μ g/mL) MTT was added to the original solution per well, and the cells continued to be cultured for 4 h. After

removing the supernatant, 150 μ L DMSO was added to each well and mixed thoroughly. Absorbance was recorded at 490 nm using a microplate reader (BIO-RAD).

CCK-8 assay

Cell viability was measured by CCK-8 assay (Beyotime, Shanghai, China) following manufacturer's instructions. Cells were cultured and treated in the same way as in the MTT assay. After the treatment, 10 μ L CCK-8 solution was added to each well and the plates were incubated for an additional 4 h at 37 °C. The absorbance at 450 nm was measured. The percentage of viable cells was calculated using the formula: ratio (%) = [OD (Treatment)-OD (Blank)]/[OD (Control)-OD (Blank)] \times 100.

Trypan blue exclusion staining

For trypan blue exclusion assay, HepG2 cells were plated in 6-well culture plates containing DMEM medium with 10% FBS and incubated at 37 °C in 5% CO₂ for 24 h and allowed to reach 60-70% confluency. The cells were then treated with the concentration approximated with IC₅₀ values of EEEO for appropriate time points (80 μ g/mL of EEEO for 12 h, 50 μ g/mL of EEEO for 24 h and 45 μ g/mL of EEEO for 48 h). The cells were then trypsinized and stained with trypan blue (Invitrogen, CA) and the viable and dead cells counted using a hemacytometer. For every sample a total of 300 cells were counted in triplicates and the percentage of viable cells was calculated using the formula: ratio (%) = the number of non-staining cells /300 \times 100.

Hoechst 33258 staining assay

The fluorescent dye Hoechst 33258 was used to visualize the nuclear fragmentation, a characteristic of apoptotic cell death (Xu *et al.*, 2013). The HepG2 cells were plated in 6-well culture plates containing DMEM medium with 10% FBS and incubated at 37 °C in 5% CO₂ for 24 h. During post-incubation stage, the cells were treated with 0, 100, 150 μ g/mL EEEO in serum-free medium for 24 h. In addition, the cells were treated with 100 μ g/mL EEEO for another 48 h. After discarding the medium, cells were washed twice with PBS, and 1.0 mL of stationary liquid (methanol: acetic acid = 3 : 1) were used to fix the cells for 30 min. And then, Hoechst 33258 solution (5 μ g/mL) was used to stain nuclei for 30 min. Finally, the nucleus shape changes were observed by fluorescence microscope (Leica Microsystems, Wetzlar, Germany).

Flow cytometry analysis (FACS)

The HepG2 cells ($1 \times 10^5 \sim 4 \times 10^5$ cells per well) were plated into 6-well cell culture plates and exposed to different concentration of EEEO (0, 100, 150 μ g/mL) for 24 h or 48 h. Cells were collected by trypsinization and centrifugation, and washed with cold PBS twice (Zheng *et al.*, 2014). Briefly, the cells were fixed with cold 80% ethanol and maintained at 4 °C for at least 18 h. Samples were then pelleted and washed with PBS. Intracellular RNA was removed by incubating samples with 1.0 mg/mL of RNaseA at 37 °C for 2 h. Finally, cells were stained with 50 μ g/mL propidium iodine (PI) and the cell cycle distribution analysis was measured using a flow cytometer (BD Biosciences, USA). Cell cycle changes were analyzed by propidium iodine staining. Cells in Sub G1 phase were considered to be apoptotic.

Reactive oxygen species (ROS) levels

The determination of ROS levels was based on the oxidation of DCFH-DA. HepG2 cells were cultivated at a density of 1×10^5 per well in a six-well plate for 24 h, and incubated with EEEO (0, 100, 150 μ g/mL) for 12 or 24 h. The cells were then treated with DCFH-DA (5 mM) for 30 min at 37 °C in the dark (Huang *et al.*, 2016). The cells were then washed twice and harvested in PBS. The fluorescence of DCFH-DA was detected with a flow cytometer.

Western blotting assay

HepG2 cells treated with EEEO (0, 100, 150 μ g/mL) were collected at different time points (0, 24 and 48 h), washed twice with ice-cold PBS, and incubated in protein lysis buffer for 30 min at 4 °C. The lysates were centrifuged at 12000 x g for 15 min at 4 °C (Feng *et al.*, 2016). The concentrations of total lysate protein were detected by a standard Bradford assay. The protein lysates were resolved by 10% sodium dodecyl sulfate-polyacrylamide gel electrophoresis and transferred to nitrocellulose membranes (Liu *et al.*, 2016). The nitrocellulose membranes were blocked with 5% non-fat milk at room temperature for 2 h and then incubated overnight at 4 °C with primary antibodies (1: 2,000 to 1: 4000 dilution). After washing the membranes three times for 10 min each with Tris-buffered saline containing Tween-20, they were incubated with HRP-conjugated secondary antibodies. Proteins were visualized using an Enhanced Chemiluminescence-Plus kit, which can analyze the expression of proteins in cells of the information

through analysis of the position of coloring and color depth for a particular protein to find the target protein.

Statistical analysis

Data are expressed as the means \pm standard deviation (SD). Statistical analyses were performed using one-way analysis of variance with Graphpad prime 5.0 software. Differences were considered statistically significant at $*P < 0.05$, $**P < 0.01$ and $***P < 0.001$ (Banafa, Roshan, 2013).

RESULTS

Chemical characterization of EEEO

EEEEO was prepared by hydro-distillation technique with a yield of 0.43% (w/w) based on the dry weight of *E. esula*. The main identified compounds, their percentages as well as the retention times were shown and listed in Figure 1 and Table I. In the case of *E. esula*, 13 different compounds were identified representing the 93.4% of the total oil. EEEO was dominant by nonacosane (19.57%), 3 α -cholesta-4,6-dien-3-ol (11.19 %) and pentacosane (10.54%), followed by eicosane (7.88%), heptacosane (7.21%), hexacosane (6.56%), phytol (5.78%) and 6,10,14-trimethyl-2-peantadecanone (5.57%). Small amounts of other chemical components were characterized as 5-hydroxy-2,4-di-t-butylphenyl pentanoic acid (4.58%), tetracosane (4.48%), and androst-5,7-dien-3-ol-17-one

(4.27%) as well as 2,6,10-trimethyl-dodecane (3.54%) and 2-(*E*)-decenal (2.25%).

Selective inhibition of cells proliferation by EEEO

The effects of EEEO on proliferation of several HCC cell lines and normal liver cell line were examined by MTT assay, CCK-8 assay and trypan blue exclusion staining. In both MTT assay and CCK-8 assay, after incubating for 24 h, viability of all HCC cell lines in EEEO treated groups were significantly inhibited in a dose-dependent manner, while EEEO treatment showed little toxic impact on normal liver cell line (L0-2). It is suggesting that EEEO inhibited proliferation of HCC. Comparison of cell viability in 4 tumor cell lines: Huh7, Hep3B, SMMC-7721 and HepG2 revealed that HepG2 cells showed the greatest sensitivity to EEEO (Figure 2A, C). Therefore, HepG2 cells were chosen as a model cell line to study mechanisms that mediate anti-HCC effects of EEEO. Based on the cell viability results, EEEO was added to 96-well plate in the concentration range of 0 to 150 $\mu\text{g/mL}$. Following culture for 12, 24 and 48 h, cell viability was measured by MTT assay and CCK-8 assay and expressed as a percentage of the control (0 $\mu\text{g/mL}$ of EEEO served as the control group) (Figure 2B, D). Progressive increase in the length of culture time increased the inhibitory effects of EEEO on HepG2 cells. These results showed that EEEO inhibited the growth of HepG2 cells in a dose- and time-dependent manner. To directly verify the anti-proliferative effects and toxicity of EEEO, HepG2 and L0-2 cells were treated

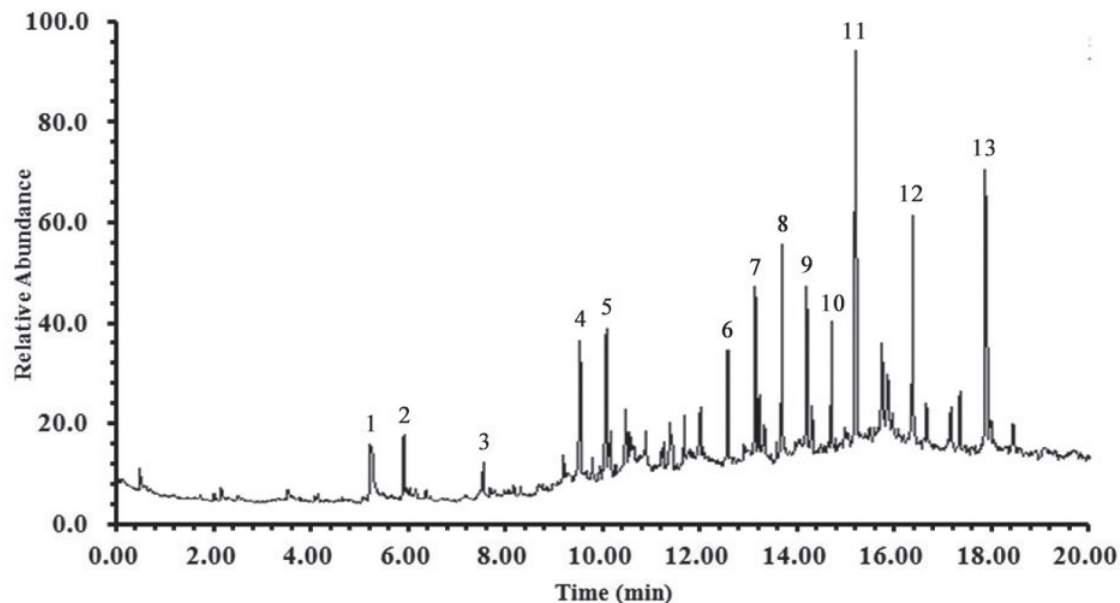


FIGURE 1 - The GC-MS analysis of EEEO is shown at different time with peak labeling corresponding to compounds 1-13.

TABLE I - Main chemical components (%) of EEEO

No	Rt (min)	Compound	Percentage (%)
1	5.21	2-(<i>E</i>)-decenal	2.25
2	5.93	2,6,10-trimethyl-dodecane	3.54
3	7.55	5-hydroxy-2,4-di- <i>t</i> -butylphenyl pentanoic acid	4.58
4	9.58	6,10,14-trimethyl-2-peantadecanone	5.57
5	10.09	phytol	5.78
6	12.48	tetracosane	4.48
7	13.20	heptacosane	7.21
8	13.61	eicosane	7.88
9	14.32	hexacosane	6.56
10	14.78	androst-5,7-dien-3-ol-17-one	4.27
11	15.20	nonacosane	19.57
12	16.39	pentacosane	10.54
13	17.97	3 α -cholesta-4,6-dien-3-ol	11.19

Rt refers to the retention time.

with EEEO in the concentrations approximated with IC_{50} values, and the percentage of viable cells was measured by trypan blue exclusion staining (Figure 2E). Similar results were obtained that EEEO significantly induced HepG2 cell death with little effect on non-tumor liver cells. These results revealed that EEEO is a promising antineoplastic agent for selectively inhibiting HCC.

EEEO-induced HepG2 cell apoptosis *in vitro*

Further experiments using fluorescence microscopy and flow cytometry analyses were performed to determine whether EEEO promotes HepG2 cell apoptosis. Morphological analysis with Hoechst 33258 staining showed nuclear with chromatin condensation and uneven staining, chromatin marginalization, and the formation of apoptotic bodies in cells. Moreover, fluorescence was more conspicuous in cells treated with 100 μ g/mL EEEO than those treated with 50 μ g/mL (Figure 3A). There was a linear increase between incubation time and fluorescence (Figure 3B). To evaluate the ability of EEEO to induce cell apoptosis, HepG2 cells were treated with 50 and 100 μ g/mL EEEO. After 24 h, the ratio of Sub-G1 DNA to the total cell population was tested by FACS. From left to right in Figure 3C, the percentages of in Sub G1 phase cells were 0.89%, 27.34% and 35.01% at 0, 50 and 100 μ g/mL, respectively, suggesting that EEEO dose-dependently led to HepG2 cell apoptosis. Similarly, EEEO time-dependently triggered HepG2 cell apoptosis (Figure 3D). These data suggested that EEEO could promote HepG2 cell apoptosis *in vitro*.

EEEO treatment caused generation of intracellular ROS

Reactive oxygen species (ROS) are usually generated in cells as by-products of metabolic reactions and their level is very high in cancer cells. Thus, cancer cells experience higher oxidative stress conditions and are prone to cell damage and death following an increase in endogenous ROS levels. In HepG2 cells, accumulating evidence indicates that intracellular ROS can trigger apoptosis (Mi *et al.*, 2016). After treatment of HepG2 cell with EEEO, the histogram peak shifted from left to the right (Figure 4A and 4B). EEEO treatment was statistically significant compared to the untreated control. ROS levels increased in a dose- and time-dependent manner.

Inhibition of mitochondrial pathway by EEEO treatment

This study suggested that it is the Bcl-2/Bax ratio that governs apoptotic signal transduction. Since the Bcl-2/Bax ratio is regulated by the release of cytochrome c from the mitochondria, the possible involvement of the Bcl-2 family proteins in the EEEO mediated apoptosis of HepG2 cells was investigated. As shown in Figure 5, Bcl-2/Bax protein ratio was decreased in EEEO-treated cells compared with the control group. Furthermore, the data indicated that EEEO could significantly increase caspase-9 expression. Caspase-9 is one of the key regulators in the mitochondrial apoptotic pathway. The activated caspase-9 is released from mitochondria, which

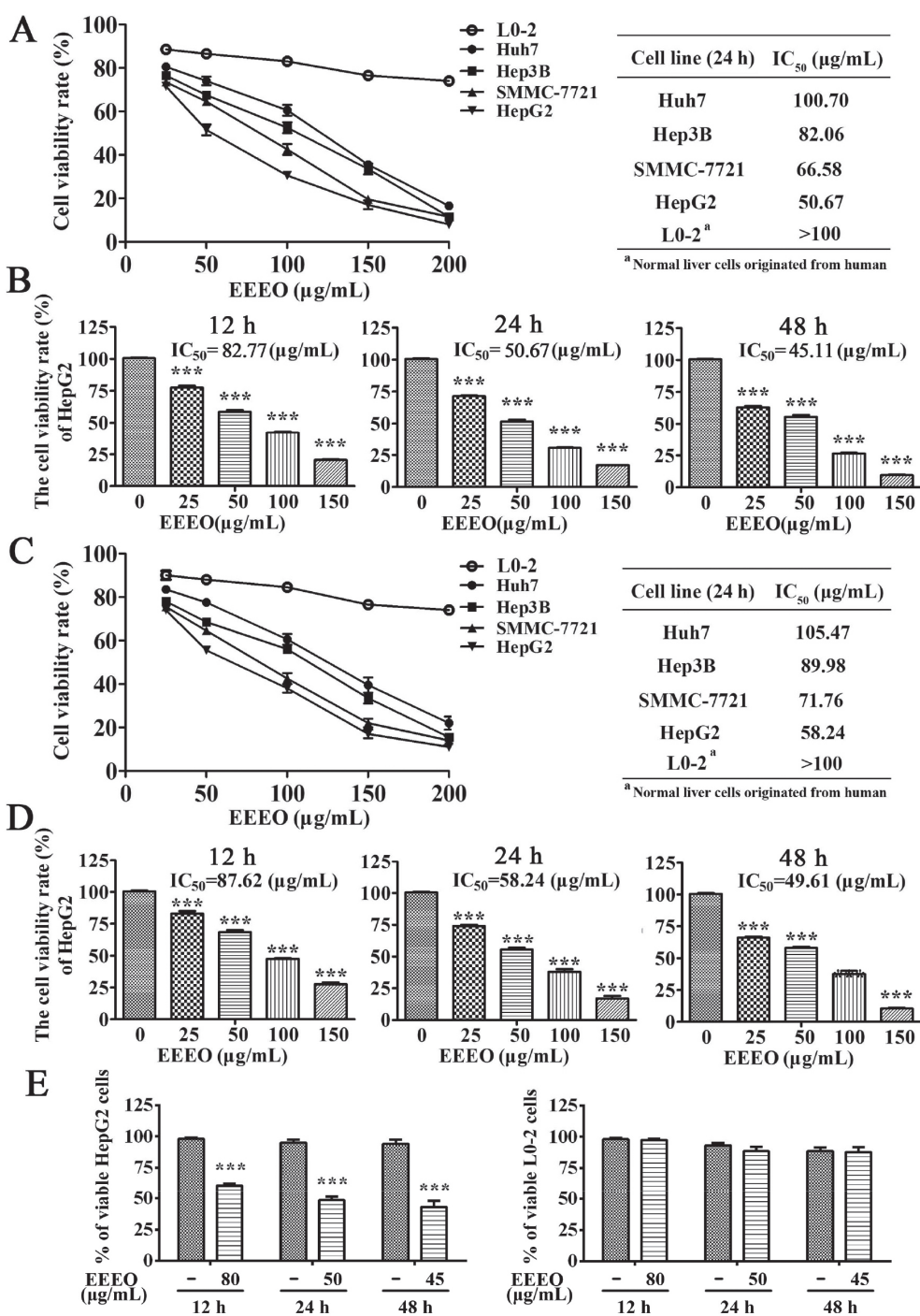


FIGURE 2 - Selective inhibitory effects of EEEO on cells proliferation. (A, B) In MTT assay, EEEO treatment inhibited HCC cells proliferation, but did not induce anti-proliferation in normal liver cells. HepG2 cells showed the most sensitive to EEEO treatment and were inhibited in a time- and dose-dependent manner. Hepatocellular carcinoma cell lines (Huh7, Hep3B, SMMC-7721 and HepG2) and normal liver cell line (L0-2) were treated with 0-150 μg/mL of EEEO for 24 h, and IC₅₀ values were calculated by MTT assay. The most sensitive cell line was further tested with above concentrations of EEEO for 12 h, 24 h and 48 h. (C, D) IC₅₀ values were also calculated by CCK-8 assay in above cell lines. Similarly, HepG2 cells were sensitive to EEEO, and showed time and dose-dependent inhibition by EEEO. (E) To verify the anti-proliferative effects and toxicity of EEEO, HepG2 and L0-2 cells were treated with EEEO whose concentrations were approximated with IC₅₀ values, and trypan blue exclusion staining was performed to measure the percentage of viable cells. In above assay, 0 μg/mL (or labeled as -) of EEEO served as control group. The data is shown as the means ± SD from three independent experiments. Asterisk denote a response that is significantly different from the control (***) $P < 0.001$.

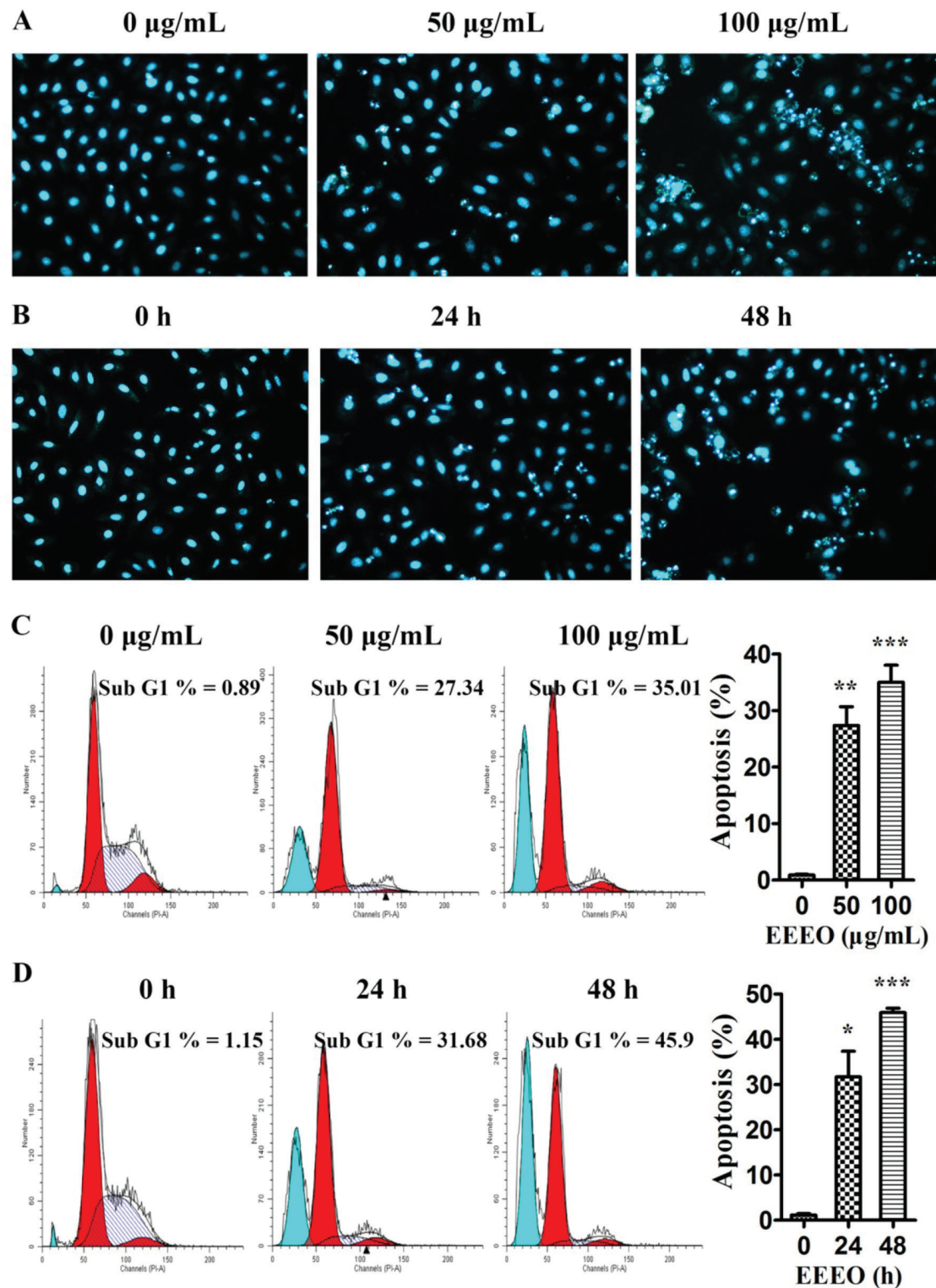


FIGURE 3 - EEEO dose- and time- dependently provoked human HepG2 cell apoptosis *in vitro*. (A) HepG2 cells were treated with 0, 50 and 100 µg/mL of EEEO. After 24 h, cell was observed under phase contrast microscope. (B) As time grows (0, 24 and 48 h), cells were also observed under phase contrast microscope (50 µg/mL of EEEO). (C) HepG2 cells were treated with 0, 50 and 100 µg/mL of EEEO for 24 h. Then, cell apoptosis was observed by FACS. (D) HepG2 cells were treated with 100 µg/mL EEEO for 0, 24 and 48 h times. Then, cell apoptosis was examined by FACS. 0 µg/mL (or 0 h) of EEEO treatment served as control group. The data are shown as the means \pm SD from three independent experiments. * $P < 0.05$, ** $P < 0.01$ and *** $P < 0.001$ vs. control. Results are representative of three independent tests.

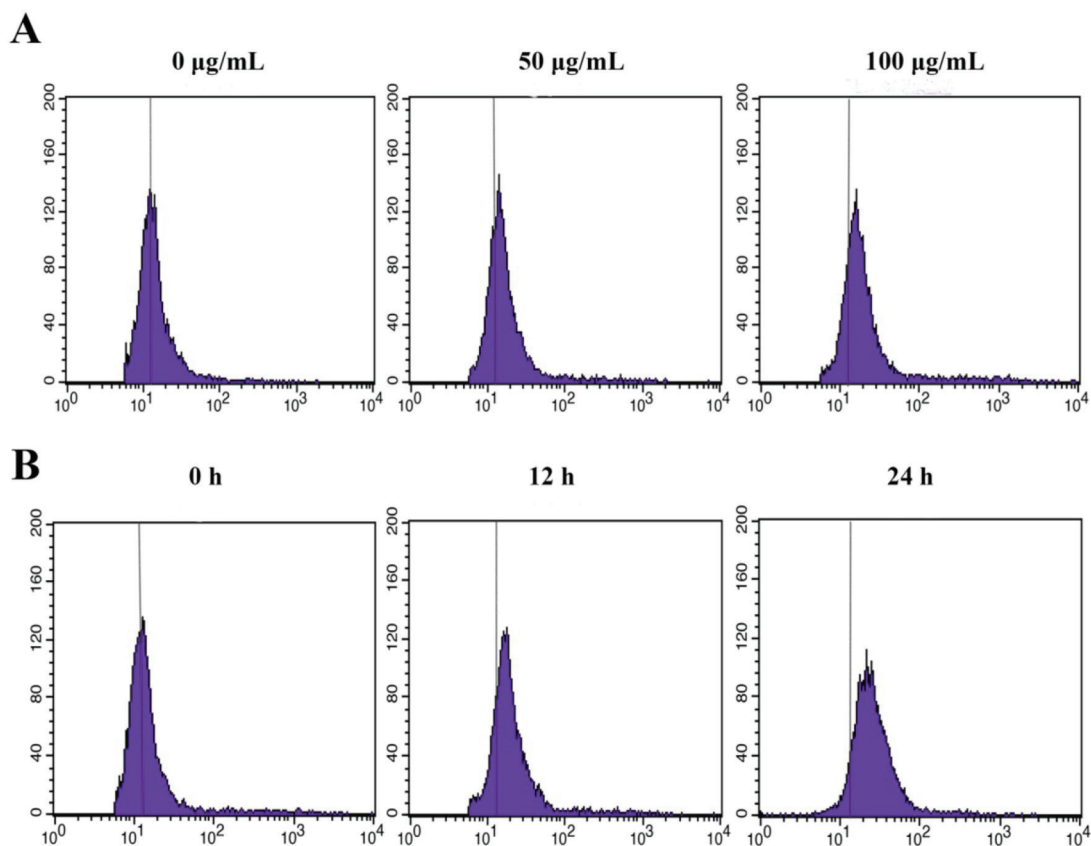


FIGURE 4 - The changes in the accumulation of ROS. (A) EEEO induced increase of ROS in dose-dependent manners. (B) HepG2 cells were treated with 50 µg/mL EEEO for 0 h, 12 h and 24 h.

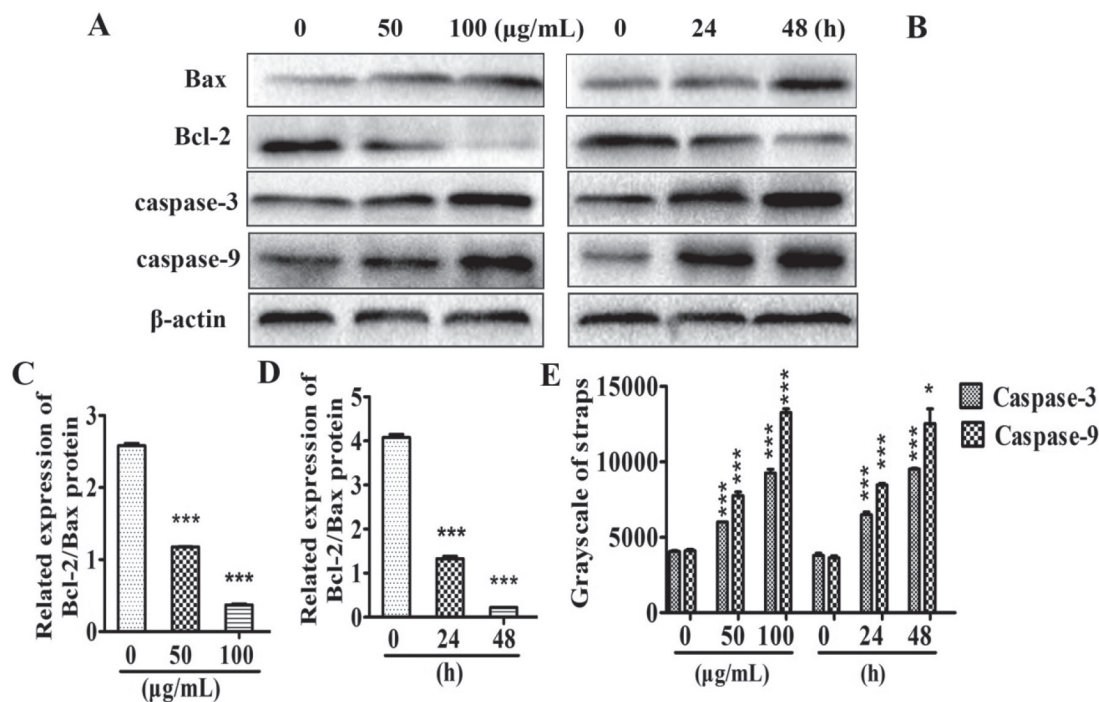


FIGURE 5 - (A) HepG2 cells were cultivated with 0, 50 and 100 µg/mL of EEEO for 24 h, and (B) incubated for 0, 24 and 48 h with 50 µg/mL of EEEO, respectively. And then Bax, Bcl-2, caspase-3, caspase-9 and β-actin were assessed via Western blotting. (C, D) Bcl-2/Bax ratio and (E) quantification of caspase-3 and caspase-9 were analyzed and expressed. 0 µg/mL (or 0 h) of EEEO treatment served as control group. Statistical analysis was tested at significance * $P < 0.05$ and *** $P < 0.001$ compared to untreated control.

then triggers executioner caspase-3, leading to apoptosis. Collectively, these data showed that EEEO could activate the expression of caspase-3 and caspase-9 and down-regulate Bcl-2/Bax expression, leading to apoptosis in HepG2 cells mediated by the mitochondrial-dependent pathway.

DISCUSSION

Since the beginning of the century, the exploration and research of natural medicine has increased in popularity (Bauer, Brönstrup, 2014). Chinese herbal medicines are rich in natural resources consisting of beneficial components with diverse chemical structures, a wide anticancer spectrum with little side effects, and low developmental costs (Ergil, Kramer, Ng, 2002). It has continued to receive domestic and foreign medical attention. Looking for effective components in natural products to treat diseases tends to become international.

The present study has shown that an essential oil extract from *E. esula* (EEEEO), considered as a Chinese herbal medicine, induced hepatocyte apoptosis in a liver cancer cell line (Whelan, Ryan, 2003). However, the potential anti-cancer mechanism of *E. esula* is not fully understood. This study examined the cell viability of EEEEO in HepG2 cell line by MTT assay, CCK-8 assay, trypan blue exclusion test and Hoechst33528 staining. The results showed that EEEEO selectively inhibited proliferation of HepG2 cells in a time- and dose-dependent manner without observable toxicity on normal liver cells. As an important mechanism mediating cell death, apoptosis is well known to be involved in the process of HCC. Consequently, cell cycle analysis indicated that EEEEO arrested cell cycle at the G0/G1 transition and induced HepG2 cell apoptosis.

Acting as signaling molecules, ROS plays a key role in physiological processes, including host defense, aging, and cellular homeostasis (Ray, Huang, Tsuji, 2012). Several studies to date have suggested that novel therapeutic strategies can be developed to preferentially inhibit cancer cell growth by increasing ROS generation. For example, the drug tempol suppresses growth of existing tumors by inhibiting proliferation and inducing apoptosis (Han, Park, 2012). In the present study, we found that EEEEO significantly increased ROS levels in dose-dependent manner, revealing that ROS may be related to the apoptosis in HepG2 cells induced by EEEEO.

Apoptosis can be initiated via 2 alternative signaling pathways: the mitochondrial-mediated intrinsic apoptotic pathway and the death receptor-mediated extrinsic apoptotic pathway (Lin *et al.*, 2008). Mitochondrial

apoptosis pathways can be initiated by intracellular stimuli and by the Bcl-2 family proteins that act as sensors to integrate death and survival signals (Yang *et al.*, 2015). The ratio of Bcl-2/Bax is a pivotal determinant, and its reduction leads to an increase in mitochondrial outer membrane permeabilization, which in turn leads to the activation of caspase-3 and caspase-9, finally triggering activation of caspase cascades culminating in cellular fragmentation (Zhao *et al.*, 2015). *E. esula* extract has been reported to inhibit proliferation and induce apoptosis in SGC-7901 cells, in a caspase-dependent manner, involving upregulation of Bax and downregulation of Bcl-2 (Fu *et al.*, 2016). To determine which apoptosis-related proteins are regulated by EEEEO in HepG2, the expression of Bax, Bcl-2, Caspase-3 and Caspase-9 proteins were analyzed using western blotting methods. The data showed that EEEEO down-regulated Bcl-2/Bax protein ratio in HepG2 cells suggesting that EEEEO promoted apoptosis of HepG2 cells. It is likely that the decrease in Bcl-2/Bax protein ratio could induce caspase-dependent mitochondrial apoptosis.

ACKNOWLEDGMENTS

We thank Accdon and Dr. Mohammad Omar Faruque for the linguistic assistance during the preparation of this manuscript.

CONFLICT OF INTEREST STATEMENT

The authors declare no competing interests.

SUPPORT

This project was financially supported by the Talent Introduction Project of Hangzhou Medical College, Zhejiang Province, China (No.2015B08), the Natural Science Foundation of Hubei Province of China (No.2017CFB517), Open Project Fund of Hubei Province Key Laboratory of Occupational Hazard Identification and Control (No. OHIC2017G03) and National Natural Science Foundation of China grants (No. 81573561 and No. 81573239).

REFERENCES

Banafa A M, Roshan S. Fucoïdan induces G1 phase arrest and apoptosis through caspases-dependent pathway and ROS induction in human breast cancer MCF-7 cells. *J Huazhong Univ Sci Technol Med Sci.* 2013;33(5):717-724.

- Bauer A, Brönstrup M. Industrial natural product chemistry for drug discovery and development. *Nat Prod Rep*. 2014;31(1):35-60.
- Chen SL, Gilbert MG. *Flora of China*. Science, Beijing and Missouri Botanical Garden Press, St Louis; 2006.
- Ernst M, Grace OM, Saslis-Lagoudakis CH, Nilsson N, Simonsen HT, Rønsted N, et al. Global medicinal uses of *Euphorbia L.* (Euphorbiaceae). *J Ethnopharmacol*. 2015;176:90-101.
- Ergil KV, Kramer EJ, Ng AT. Chinese herbal medicines. *Western J Med*. 2002;176(4):275-279.
- Feng X, Yu W, Zhou F, Chen J, Shen P. A novel small molecule compound diaporine inhibits breast cancer cell proliferation via promoting ROS generation. *Biomed Pharmacother*. 2016;83:1038-1047.
- Fu ZY, Han XD, Wang AH, Liu XB. Apoptosis of human gastric carcinoma cells induced by *Euphorbia esula latex*. *World J Gastroenterol*. 2016;22(13):3564-3572.
- Hong YP, Li ZD, Prasoon P, Zhang Q. Immunotherapy for hepatocellular carcinoma: From basic research to clinical use. *World J Hepatol*. 2015;7(7):980-992.
- Huang J, Zhou C, He J, Hu Z, Guan WC, Liu SH. Protective effect of reduced glutathione C60. *J Huazhong Univ Sci Technol Med Sci*. 2016;36(3):356-363.
- Han YH, Park WH. Tempol inhibits growth of As4.1 juxtglomerular cells via cell cycle arrest and apoptosis. *Oncol Rep*. 2012;27(3):842-848.
- Li XQ, Ling CQ. Chinese herbal medicine for side effects of transarterial chemoembolization in liver cancer patients: a systematic review and meta-analysis. *Chin J Integr Med*. 2012;10(12):1341-1362.
- Li Y, Liu B, Yang F, Yu Y, Zeng A, Ye T, et al. Lobaplatin induces BGC-823 human gastric carcinoma cell apoptosis via ROS-mitochondrial apoptotic pathway and impairs cell migration and invasion. *Biomed Pharmacother*. 2016;83:1239-1246.
- Liu B, Lei M, Hu T, Yu F, Xiao DM, Kang H. Inhibitory effects of SRT1720 on the apoptosis of rabbit chondrocytes by activating SIRT1 via p53/bax and NF- κ B/PGC-1 α pathways. *J Huazhong Univ Sci Technol Med Sci*. 2016;36(3):350-355.
- Lin Y, Shi R, Wang X, Shen HM. Luteolin, a flavonoid with potential for cancer prevention and therapy. *Curr Cancer Drug Targets*. 2008;8(7):634-646.
- Lv D, Guo KW, Xu C, Huang M, Zheng SJ, Ma XH, et al. Essential oil from *Siegesbeckia pubescens* induces apoptosis through the mitochondrial pathway in human HepG2 Cells. *J Huazhong Univ Sci Technol Med Sci*. 2017;37(1):87-92.
- Mi Y, Xiao C, Du Q, Wu W, Qi G, Liu X. Momordin Ic couples apoptosis with autophagy in human hepatoblastoma cancer cells by reactive oxygen species (ROS)-mediated PI3K/Akt and MAPK signaling pathways. *Free Radical Bio Med*. 2016;90:230-242.
- Ray PD, Huang BW, Tsuji Y. Reactive oxygen species (ROS) homeostasis and redox regulation in cellular signaling. *Cell Signal*. 2012;24(5):981-990.
- Santos MS, Abreu PH, García-Laencina PJ, Simão A, Carvalho A. A new cluster-based oversampling method for improving survival prediction of hepatocellular carcinoma patients. *J Biomed Inform*. 2015;58:49-59.
- Song P, Xu C, Ma YR, Lv J, Yang J, Wang C, Yang X. In vitro anti-hepatoma screening of 100 commonly used Tibetan medicines. *J South Central Univ National (Nat Sci Edition)*. 2015a;34(2):64-67.
- Song P, Wang Q, Lv J, Xu C, Lin QX, Ma XH, et al. HPLC-based activity profiling of anti-hepatocellular carcinoma constituents from the Tibetan medicine, *Caragana tibetica*. *J Huazhong Univ Sci Technol Med Sci*. 2015b;35(3):450-455.
- Stepanenko AA, Dmitrenko VV. Pitfalls of the MTT assay: direct and off-target effects of inhibitors can result in over/underestimation of cell viability. *Gene*. 2015;574(2):193-203.
- Wei KR, Yu X, Zheng RS, Peng X-B, Zhang S-W, Ji M-F, et al. Incidence and mortality of liver cancer in China, 2010. *Chin J Cancer*. 2014;33(8):388-94.
- Whelan LC, Ryan MF. Ethanolic extracts of *Euphorbia* and other ethnobotanical species as inhibitors of human tumor cell growth. *Phytomedicine*. 2003;10(1):53-58.
- Xu M, Hong M, Xie H. Histone deacetylase inhibitors induce human renal cell carcinoma cell apoptosis through p-JNK activation. *J South Med Univ*. 2013;33(10):1409-1415.

Yang X, Huang M, Zheng S, Ma X, Wan D, Feng Y, et al. Liquid chromatography with mass spectrometry and NMR spectroscopy based discovery of cytotoxic principles from *Daphne tangutica* Maxim. *J Sep Sci*. 2016;39(11):2179-2187.

Yang X, Huang M, Cai J, Lv D, Lv J, Zheng S, et al. Chemical profiling of anti-hepatocellular carcinoma constituents from *Caragana tangutica* Maxim. by off-line semi-preparative HPLC-NMR. *Nat Prod Res*. 2017;31(10):1150-1155.

Yang L, Cui Y, Shen J, Lin F, Wang X, Long M, et al. Antitumor activity of SA12, a novel peptide, on SKBr-3 breast cancer cells via the mitochondrial apoptosis pathway. *Drug Des Dev Ther*. 2015;9:1319-1330.

Zheng Q, Liu W, Li B, Chen HJ, Zhu WS, Yang GX, et al. Anticancer effect of icaritin on human lung cancer cells through inducing S phase cell cycle arrest and apoptosis. *J Huazhong Univ Sci Technol Med Sci*. 2014;34(4):497-503.

Zhao W, Yang Y, Zhang YX, Zhou C, Li HM, Tang YL, et al. Fluoride-containing podophyllum derivatives exhibit antitumor activities through enhancing mitochondrial apoptosis pathway by increasing the expression of caspase-9 in HeLa cells. *Sci Rep*. 2015;5:17175.

Received for publication on 17th September 2017

Accepted for publication on 17th October 2018